

# Adding Salt to an Aqueous Solution of t-Butanol: Is Hydrophobic Association Enhanced or Reduced?

Dietmar Paschek,<sup>1,\*</sup> Alfons Geiger,<sup>1</sup> Momo Jeufack Hervé,<sup>2</sup> and Dieter Suter<sup>2</sup>

<sup>1</sup>*Physikalische Chemie und*

<sup>2</sup>*Fachbereich Physik, Universität Dortmund, D-44227 Dortmund, Germany*

(Dated: May 24, 2019)

Recent neutron scattering experiments on aqueous salt solutions of amphiphilic t-butanol by Bowron and Finney [Phys. Rev. Lett. **89**, 215508 (2002); J. Chem. Phys. **118**, 8357 (2003)] suggest the formation of t-butanol pairs, bridged by a chloride ion via  $\text{O}-\text{H}\cdots\text{Cl}^-$  hydrogen-bonds, and leading to a reduced number of intermolecular hydrophobic butanol-butanol contacts. Here we present a joint experimental/theoretical study on the same system, using a combination of molecular dynamics simulations and nuclear magnetic relaxation measurements. Both theory and experiment clearly support the more intuitive scenario of an enhanced number of hydrophobic contacts in the presence of the salt, as it would be expected for purely hydrophobic solutes [J. Phys. Chem. B **107**, 612 (2003)]. Although our conclusions arrive at a structurally completely distinct scenario, the molecular dynamics simulation results are within the experimental errorbars of the Bowron and Finney work.

## I. INTRODUCTION

Nonpolar solutes, such as noble gases or alkanes, don't like to be dissolved in water. Consequently, they are considered as "hydrophobic" and their corresponding solvation free energy is found to be large and positive [1, 2, 3, 4, 5]. This effect is typically found to be significantly strengthened when salt is added, leading to a further reduced solubility of hydrophobic species such as noble gases, or methane [6, 7]. The increasing excess chemical potential is usually found to be proportional to the salt concentration over large concentration ranges and is therefore parameterized in terms of Setschenow's concentration independent salting out coefficient [6]. In line with the observation of an increased positive solvation free energy upon addition of salt, Ghosh et al. [8] report an increased number of hydrophobic contacts in a diluted aqueous solution of methane. Moreover, for the case of hydrophobic interactions in a hydrophobic polymer chain, an approximately linear relationship between the salt concentration and the strength of pairwise hydrophobic interactions has been determined [9]. This observation seems to be in line with the general finding of Koga et al., that the excess chemical potential of a small hydrophobic particle and the strength of hydrophobic pair interactions appears to be (almost) linearly related [5, 10].

However, purely hydrophobic compounds are probably not very typical representatives of biophysical constituents. Usually, proteins and membrane-forming lipids are amphiphilic in the sense that they are composed of both, hydrophobic and hydrophilic groups, where the latter ones ensure a sufficiently high solubility in an aque-

ous environment. In addition, the delicate interplay between hydrophobicity and hydrophilicity is exploited by nature to predetermine the dimensions of molecular aggregates in aqueous solution [11, 12, 13]. Small amphiphilic alcohols might thus be considered as a minimalist model system to explore the subtle interplay between hydrophobic and hydrophilic effects. Numerous experimental studies on alcohol aggregation in aqueous solution have been reported, based on nuclear magnetic resonance [14, 15, 16, 17, 18], as well as light-, x-ray-, and neutron scattering techniques [19, 20, 21, 22, 23, 24, 25].

Salts are known to influence a number of properties of aqueous solutions in a systematic way [26]. The effect of different anions and cations appears to be ordered in a sequence, already proposed by Hofmeister in 1888 [27], deduced from a series of experiments on the salts ability to precipitate "hen-egg white protein". However, the exact reason for the observed specific cation and anion sequences is still not completely understood, since the same salt that can precipitate a protein at one concentration can "salt it in" at another [28]. Model calculations [29], as well as nuclear magnetic relaxation experiments [15] propose a delicate balance between ion adsorption and exclusion at the solute interface, tuned by the solvent (water) structure modification according to the ion hydration [30, 31] and hence possibly subject to molecular details.

Recently, Bowron and Finney provided a detailed mechanistic picture of the possible salting out process of t-butanol (TBA) in aqueous solution. The atomistic structure of the solution was determined from neutron scattering experiments [24, 25], varying solute and solvent isotopic compositions [32]. Their analysis relies largely on the accuracy of the employed empirical potential structure refinement (EPSR) technique of Soper [33, 34]. Their main observation is that TBA-molecules form dimers that are connected by hydrogen bonds to a central chloride anion. Salting out appears hence due to the formation of anion-bridged solute-solute aggre-

---

\*Electronic address: dietmar.paschek@udo.edu;  
URL: <http://ganter.chemie.uni-dortmund.de/~pas>; Fax:  
+49-231-755-3937

gates, increasing the solutes overall hydrophobic surface and thus reducing the solubility of the whole complex [35, 36, 37]. A straightforward conjecture would suggest that the salting out of proteins could be driven by analogous anion-bridged aggregates. We would like to point out that the proposed mechanism has remarkable similarity with the “differential hydrophobicity” concept of Burke et al. [38] used to explain the specific protein-aggregation behavior observed in Huntington’s disease.

The molecular dynamics simulations discussed here, however, do not show any evidence for a “salting out”-scenario as proposed by Bowron and Finney. Moreover, upon addition of salt we find an increased number of hydrophobic contacts of the TBA molecules which increases with higher salt concentration. Using a combination of molecular dynamics simulations and nuclear magnetic relaxation experiments we show that an association parameter based on NMR measurable quantities and introduced by H.G. Hertz et al. [39, 40] is a useful measure for the association of TBA molecules in the present case. Both theory and NMR experiments consistently support the simpler picture of an enhancing hydrophobic association in the case of aqueous TBA/salt solutions.

## II. METHODS

### A. Dipolar nuclear magnetic relaxation and correlations in the structure and dynamics of aqueous solutions

The molecular dynamics simulations yield the time-dependent positions of the atomic nuclei. Experimentally, the individual molecular positions are not available. However, a useful measure of molecular association is experimentally accessible via the measurement of nuclear spin relaxation rates and is discussed in a separate section below. In this section we would like to briefly summarize the underlying theory.

The most important contribution to the relaxation rate of nuclear spins  $I = 1/2$  is the magnetic dipole-dipole interaction. The relaxation rate, i.e. the rate at which the nuclear spin system approaches thermal equilibrium, is determined by the time dependence of the magnetic dipole-dipole coupling. For two like spins, it is [41]

$$T_1^{-1} = 2\gamma^4\hbar^2 I(I+1)(\mu_0/4\pi)^2 \left\{ \int_0^\infty \left\langle \sum_j^N \frac{D_{0,1}[\Omega_{ij}(0)]}{r_{ij}^3(0)} * \frac{D_{0,1}[\Omega_{ij}(t)]}{r_{ij}^3(t)} \right\rangle e^{i\omega t} dt + 4 \int_0^\infty \left\langle \sum_j^N \frac{D_{0,2}[\Omega_{ij}(0)]}{r_{ij}^3(0)} * \frac{D_{0,2}[\Omega_{ij}(t)]}{r_{ij}^3(t)} \right\rangle e^{i2\omega t} dt \right\}, \quad (1)$$

where  $D_{k,m}[\Omega]$  is the  $k, m$ -Wigner rotation matrix element of rank 2. The Eulerian angles  $\Omega(0)$  and  $\Omega(t)$  at time zero and time  $t$  specify the dipole-dipole vector relative to the laboratory fixed frame of a pair of spins and

$r_{ij}$  denotes their separation distance and  $\mu_0$  specifies the permittivity of free space. The sum indicates summation of all  $j$  interacting like spins in the entire system. For the case of an isotropic fluid and in the extreme narrowing limit Eq. (1) simplifies to [42]

$$T_1^{-1} = 2\gamma^4\hbar^2 I(I+1) \left( \frac{\mu_0}{4\pi} \right)^2 \int_0^\infty G_2(t) dt. \quad (2)$$

The dipole-dipole correlation function here is abbreviated as  $G_2(t)$  and is available through [42, 43]

$$G_2(t) = \left\langle \sum_j r_{ij}^{-3}(0) r_{ij}^{-3}(t) P_2[\cos \theta_{ij}(t)] \right\rangle, \quad (3)$$

where  $\cos \theta_{ij}(t)$  is the angle between the vectors  $\vec{r}_{ij}$  joining spins  $i$  and  $j$  at time 0 and at time  $t$  [42] and  $P_2$  is the second Legendre polynomial.

To calculate the integral, we separate the correlation function  $G_2(t)$  into an  $r^{-6}$ -prefactor, which is sensitive to the structure of the liquid (average internuclear distances) and a correlation time  $\tau_2$ , which is obtained as the time-integral of the normalized correlation function  $\hat{G}(t)$ , and which is sensitive to the mobility of the molecules in the liquid,

$$\int_0^\infty G_2(t) dt = \left\langle \sum_j r_{ij}^{-6}(0) \right\rangle \tau_2. \quad (4)$$

The correlation function  $G_2$  and hence  $T_1$  can be calculated directly from MD-simulation trajectory data. From the definition of the dipole-dipole correlation function in Eq. (3) it follows directly that the relaxation time  $T_1$  is affected by both, reorientational and translational motions in the liquid. Moreover, it is obvious that it also depends strongly on the average distance between the spins and is hence sensitive to changing inter- and intramolecular pair distribution functions [39, 40]. In addition, the  $r^{-6}$ -weighting introduces a particular sensitivity to changes occurring at short distances. For convenience, one may divide the spins  $j$  into different classes according to whether they belong to the same molecule as spin  $i$ , or not, thus arriving at an *inter*- and *intramolecular* contribution to the relaxation rate

$$T_1^{-1} = T_{1,\text{inter}}^{-1} + T_{1,\text{intra}}^{-1}, \quad (5)$$

which are determined by corresponding intra- and intermolecular dipole-dipole correlation functions  $G_{2,\text{intra}}$  and  $G_{2,\text{inter}}$ . The intramolecular contribution is basically due to molecular reorientations and conformational changes and has been used extensively to study the reorientational motions, such as that of the H-H-vector in CH<sub>3</sub>-groups in molecular liquids and crystals [44]. In the course of this paper, however, we are particularly interested in the association of solute molecules, and will

therefore focus on the intermolecular contribution (see also experimental section).

The structure of the liquid can be expressed in terms of the intermolecular site-site pair correlation function  $g_{ij}(r)$ , describing the probability of finding a second atom of type  $j$  in a distance  $r$  from a reference site of type  $i$  according to [45]

$$g_{ij}(r) = \frac{1}{N_i \rho_j} \left\langle \sum_{k=1}^{N_i} \sum_{l=1}^{N_j} \delta(\vec{r} - \vec{r}_{kl}) \right\rangle, \quad (6)$$

where  $\rho_j$  is the number density of atoms of type  $j$ . The prefactor of the intermolecular dipole-dipole correlation function is hence related to the pair distribution function via an  $r^{-6}$  integral of the pair correlation function

$$\left\langle \sum_j r_{ij}^{-6}(0) \right\rangle = \rho_j \int_0^\infty r^{-6} g_{ij}(r) 4\pi r^2 dr. \quad (7)$$

Since the process of enhanced association in a molecular solution is equivalent with an increase of the nearest neighbor peak in the radial distribution function, Eq. 7 establishes a quantitative relationship between the degree of intermolecular association and the intermolecular dipolar nuclear magnetic relaxation rate.

### B. Self-association: the Hertz “A”-parameter

As a measure of the degree of intermolecular association, Hertz and co-workers [39, 40, 46] introduced a so-called “association parameter  $A$ ”, which is a weighted integral of the pair correlation function of the nuclei contributing to the dipolar relaxation process (in the present case  $^1\text{H}$  nuclei in TBA-d1-solutions) and is defined as [47]:

$$A = \frac{1}{2} \frac{\gamma^4 \hbar^2}{a^4} \left( \frac{\mu_0}{4\pi} \right)^2 \int_0^\infty \left( \frac{a}{r} \right)^6 g_{HH}(r) 4\pi r^2 dr, \quad (8)$$

where  $a$  is the “closest approach distance of the interacting nuclei”. This distance, together with the correlation time  $\tau_{2,\text{inter}}$  is also related to the self-diffusion coefficient  $D$  of the solute molecules. Here it is assumed that the dipole-dipole correlation time  $\tau_{2,\text{inter}}$  and the inverse self-diffusion coefficient are linearly related via

$$D = \frac{a^2}{3\tau_{2,\text{inter}}}. \quad (9)$$

The diffusion coefficient can also be measured by NMR, using, e.g., pulse field gradient experiments.

It is usually just assumed that  $a$  is independent of the system’s composition [48]. In the present study, we can overcome part of the uncertainty, since we can calculate all quantities required for  $A$  independently from our MD simulations and determine the  $A$ -parameter for our model system exactly in the same way as it is done in the

TABLE I: Nonbonded interaction parameters used in the present study. The <sup>1</sup> refers to the ion parameter set of Heinzinger [50], whereas the <sup>2</sup> refers to the parameters of Koneshan et al. [51]. Lorentz-Berthelot mixing rules according to  $\sigma_{ij} = (\sigma_{ii} + \sigma_{jj})/2$  and  $\epsilon_{ij} = \sqrt{\epsilon_{ii} \epsilon_{jj}}$  were employed.

Site	$q/ e $	$\sigma/\text{nm}$	$\epsilon k^{-1}/\text{K}$
OW	-0.8476	3.1656	78.2
HW	+0.4238	–	–
CT	+0.265	3.50	33.2
CT(CH3)	-0.180	3.50	33.2
HC	+0.060	2.50	15.1
OH	-0.683	3.12	85.6
HO	+0.418	–	–
Na <sup>1</sup>	+1.0	2.73	43.06
Cl <sup>1</sup>	-1.0	4.86	20.21
Na <sup>2</sup>	+1.0	2.583	50.32
Cl <sup>2</sup>	-1.0	4.401	50.32

experiment. Since the TBA-TBA coordination number is also available from MD, the simulations thus provide a “proof of concept” for a system behaving closely similar to the real system.

The  $A$ -parameter is a useful measure in the sense that it is directly related to the solvent-mediated attractive or repulsive interactions between solute molecules through the sharpness, or peak-height, of the pair correlation function. The *relative* change of the local concentration of the observed molecules is identified by the *relative* change in the  $A$ -parameter: as  $g_{HH}(r)$  becomes sharper when the density of the next neighbor atoms around the reference atom increases, the  $A$ -parameter increases. Using the definitions of Eq. 8 and Eq. 9,  $A$  is given in terms of NMR measurable quantities [47, 49]:

$$A = \frac{1}{T_{1,\text{inter}}} \times \frac{D}{\rho_H}, \quad (10)$$

where  $D$  is the self-diffusion coefficient of the solute molecules and  $\rho_H$  is the number density of the  $^1\text{H}$ -nuclei in the system. Making use of the concentration dependence outlined in Eq. 10, the aggregation behavior of solvent molecules is usually available from a concentration series [17]: an enhanced association is identified by an increasing  $A$ -parameter, whereas a de-association corresponds to a decrease. In the present case, where we vary the salt concentration, we measure the change of the  $A$ -parameter with the salt concentration.

### C. MD simulation details

We employ molecular dynamics (MD) simulations in the NPT ensemble using the Nosé-Hoover thermostat [52, 53] and the Rahman-Parrinello barostat [54, 55] with

TABLE II: Parameters characterizing the performed MD-simulation runs. All simulations were carried out at  $T=298$  K and  $P=1$  bar. The star \* indicates the simulation run employing the parameters of Koneshan et al. [51] for NaCl. For comparison a pure water simulation run of 500 SPCE molecules over 20 ns was performed yielding an average density  $998.4 \text{ kg m}^{-3}$ .

$N(\text{H}_2\text{O})$	1000	1000	1000	1000
$N(\text{TBA})$	20	20	20	20
$N(\text{NaCl})$	–	10*	10	20
Simul. length $\tau/\text{ns}$	50	100	100	100
Density $\langle\rho\rangle/\text{kg m}^{-3}$	991.5	1008.6	1002.6	1013.7
$\langle c(\text{TBA})\rangle/\text{mol l}^{-1}$	1.0170	1.0044	0.9984	0.9810
$\langle c(\text{NaCl})\rangle/\text{mol l}^{-1}$	–	0.5022	0.4992	0.9810

coupling times  $\tau_T = 1.5 \text{ ps}$  and  $\tau_p = 2.5 \text{ ps}$  (assuming the isothermal compressibility to be  $\chi_T = 4.5 \cdot 10^{-5} \text{ bar}^{-1}$ ), respectively. The electrostatic interactions are treated in the “full potential” approach by the smooth particle mesh Ewald summation [56] with a real space cutoff of  $0.9 \text{ nm}$  and a mesh spacing of approximately  $0.12 \text{ nm}$  and 4th order interpolation. The Ewald convergence factor  $\alpha$  was set to  $3.38 \text{ nm}^{-1}$  (corresponding to a relative accuracy of the Ewald sum of  $10^{-5}$ ). A  $2.0 \text{ fs}$  timestep was used for all simulations and the solvent constraints were solved using the SETTLE procedure [57], while the SHAKE method was used to constrain the solute bond lengths [58]. All simulations reported here were carried out using the GROMACS 3.2 program [59, 60]. The MOSCITO suit of programs [61] was employed to generate start configurations, topology files, and was used for the entire data analysis presented in this paper. Statistical errors in the analysis were computed using the method of Flyvbjerg and Petersen [62]. For all reported systems initial equilibration runs of  $1 \text{ ns}$  length were performed using the Berendsen weak coupling scheme for pressure and temperature control ( $\tau_T = \tau_p = 0.5 \text{ ps}$ ) [63].

As in Refs. [24, 25] we study  $0.02$  mole fraction aqueous solutions of t-butanol with and without presence of sodium chloride. The simulations were carried out for  $1 \text{ bar}$  and  $298 \text{ K}$ . Our model system contains  $1000$  water molecules, represented by the three center SPCE model [64]. The flexible OPLS all-atom forcefield [65] is employed for the  $20$  TBA-molecules. Here the bond lengths were kept fixed. Ten and twenty sodium chloride ion pairs were used to represent the salt solution. In order to check the influence of ion parameters variation, the two different parameter sets according to Heinzinger [50] and Koneshan et al. [51] were employed. All non-bonded interaction parameters are summarized in Table I. To ensure proper sampling, and to allow an accurate determination of the system’s structural and dynamical properties, the aqueous TBA solutions were studied for  $50 \text{ ns}$ , whereas the salt-solutions were monitored for  $100 \text{ ns}$ . The performed simulation runs and resulting concentrations

are indicated in Table II. For comparison, a pure water system of  $500$  SPCE water molecules was simulated for  $20 \text{ ns}$  for the same conditions.

## D. Experimental Details

To experimentally determine the association behavior of TBA molecules in aqueous solutions we measured intermolecular NMR relaxation rates, self diffusion coefficients, and the densities of the aqueous solutions. All experimental data are summarized in Table III.

The observed relaxation rates depend on inter- as well as intra-molecular correlation functions. To extract the intermolecular rates, which are sensitive to the solute-solute association, we used the method of isotopic dilution [66].

Since we are interested only in the hydrophobic methyl-protons, we deuterated the water and the hydroxyl group of the TBA. Isotopic dilution was performed by mixing  $(\text{CD}_3)_3\text{COD}$  (TBA-d10) with  $(\text{CH}_3)_3\text{COD}$  (TBA-d1). We parameterize the dilution with the mole fraction

$$x_H = \frac{[\text{TBA-d1}]}{[\text{TBA-d1}] + [\text{TBA-d10}]}.$$

The basic assumption of the isotopic dilution procedure is that the relaxation rate is given by the sum of an intramolecular term, which is independent of the dilution, and an intermolecular term, which is proportional to the concentration of the corresponding molecular species. The contribution of the deuterated molecules can be taken as proportional to that of the protonated molecules, with a reduction factor [41]

$$\alpha = \frac{2}{3} \frac{\gamma_D^2}{\gamma_H^2} \frac{I_D(I_D + 1)}{I_H(I_H + 1)} = 0.042.$$

The observed relaxation rate becomes therefore

$$\frac{1}{T_1} = \frac{1}{T_{1,0}} + \frac{1}{T_{1,\text{intra}}} + \frac{1}{T_{1,\text{inter}}}[(1 - \alpha)x_H + \alpha]. \quad (11)$$

TABLE III: Experimental densities  $\rho$ , intermolecular relaxation times  $T_{1,\text{inter}}$  and self-diffusion coefficients  $D$  for TBA-d1 in TBA-d10/ $\text{D}_2\text{O}$ /NaCl solutions. All experiments were carried out at  $T=298 \text{ K}$  at ambient pressure conditions. Also given are the TBA-d1 concentrations and the obtained  $A$ -parameters.

TBA-d1: $\text{D}_2\text{O}$ :NaCl	2:100:0	2:100:1	2:200:2
$\rho/\text{kg m}^{-3}$	1083.9	1106.1	1122.5
$c(\text{TBA})/\text{mol l}^{-1}$	1.0059	0.9994	0.9882
$c(\text{NaCl})/\text{mol l}^{-1}$	–	0.5270	1.0403
$T_{1,\text{inter}}/\text{s}$	$44.89 \pm 1.74$	$41.02 \pm 4.73$	$37.92 \pm 0.13$
$D/10^{-9} \text{ m}^2 \text{ s}^{-1}$	0.3962	0.3818	0.3792
$A/10^{-39} \text{ m}^5 \text{ s}^{-2}$	1.619	1.718	1.826

Here,  $T_{1,\text{intra}}$  denotes the intramolecular contribution from protons within the methyl groups of the same molecule as the one being measured,  $T_{1,\text{inter}}$  the intermolecular contributions between different TBA molecules, and  $T_{1,0}$  all other terms, such as paramagnetic relaxation and interaction with other molecules such as  $\text{D}_2\text{O}$ . To extract the intermolecular term, we measured the relaxation rate as a function of the isotopic dilution and fitted the measured data points to Eq. 11.

The diffusion coefficients of TBA-d1 were determined from the Pulsed Gradient Spin Echo (PGSE) experiments [67], where the gradient calibration was done using the diffusion coefficient of pure water [68].

The  $^1\text{H}$  number density in the TBA-d1/ $\text{D}_2\text{O}$  and TBA-d1/ $\text{D}_2\text{O}$ /NaCl solutions was obtained by measuring the mass density of the corresponding solutions with defined composition using a commercial Anton Paar oscillating U-tube density meter.

The TBA-d1 (99%) was purchased from Cambridge Isotope laboratories, the TBA-d10 (99%) from Isotec. The solvent  $\text{D}_2\text{O}$  with the purity 99.96% was obtained from Merck KGaA. The solution was prepared by measuring the appropriate amount of each compound with a micropipette, and by weighing corresponding amount of NaCl. The degassing process was done by the usual Freeze-Pump-Thaw technique, repeated several times until no gas bubbles didn't develop from the solution. Finally, the samples were flame sealed. Relaxation and diffusion measurements were carried out at 600MHz using a Varian Infinity Spectrometer system. All experiments were conducted under controlled temperature conditions at 25°C.

### III. RESULTS AND DISCUSSION

#### A. Structural characterization of the aqueous TBA solutions

The most prominent feature of the neutron scattering work of Bowron and Finney is the observation of a significant decrease of the height of the first peak of the central-carbon pair correlation function upon addition of sodium chloride [24, 25]. This decrease of the nearest neighbor peak is accompanied by an increase at a distance of about 0.85 nm. From steric arguments and an analysis of their EPSR data, Bowron and Finney conclude that this process is according to the formation of chloride-bridged TBA-pairs. In Figure 1 we present the corresponding curves obtained from the present MD simulations. Surprisingly, exactly the opposite behavior is found. Upon addition of salt a notable increase of the first peak is observed, suggesting an enhanced TBA-TBA aggregation. Moreover, this increase is clearly more pronounced when increasing the salt concentration from about 0.5 molar to about 1 molar. Table IV provides a quantitative analysis of the pair correlation data in terms of coordination

numbers

$$N_{\alpha\beta} = 4\pi\rho_\beta \int_{r_{\min}}^{r_{\max}} r^2 g_{\alpha\beta}(r) dr, \quad (12)$$

where  $\rho_\beta$  is the average number density of atom type  $\beta$ . In order to provide comparability with the data obtained by Bowron and Finney, the values of  $r_{\min}$  and  $r_{\max}$  for the distance intervals given in Table IV were taken from Ref. [25]. As the increasing peak height of the MD-data suggests, the TBA-TBA coordination number increases with increasing salt concentration. Moreover, the increase is found to be significantly larger than the size of the associated errorbars.

A more detailed picture of the structure of the aqueous salt solutions of TBA is given in terms of selected solute/solvent pair correlation functions in Figure 2. In order to take the amphiphilic nature of TBA more properly into account we also provide two-dimensional cylindrical pair correlation functions  $g(z, r)$ , indicating the arrangement of molecules around a central TBA molecule using the notation of [45]

$$g(r, z) = \frac{1}{N_{\text{TBA}}\rho_\beta} \left\langle \sum_{i=1}^{N_{\text{TBA}}} \sum_{j=1}^{N_\beta} \delta(z - \vec{n}_{\text{OH}}\vec{r}_{ij}) \times \delta\left(r - \sqrt{r_{ij}^2 - (\vec{n}_{\text{OH}}\vec{r}_{ij})^2}\right) \right\rangle \quad (13)$$

where the  $z$ -axis is aligned along the TBA intramolecular unit-vector  $\vec{n}_{\text{OH}} = \vec{r}_{\text{OH}}/r_{\text{OH}}$  pointing from the center of mass to the hydroxyl oxygen. The index  $i$  runs over all TBA molecules, whereas the index  $j$  runs over a particular subset of molecules (TBA, anions, or cations). The vector  $\vec{r}_{ij} = \vec{r}_j - \vec{r}_i$  represents the center of mass separation between particles  $i$  and  $j$ . The schematic shown in Figure 3 illustrates how the parameters  $r$  and  $z$  are defined. The 2d-distribution of TBA molecules around

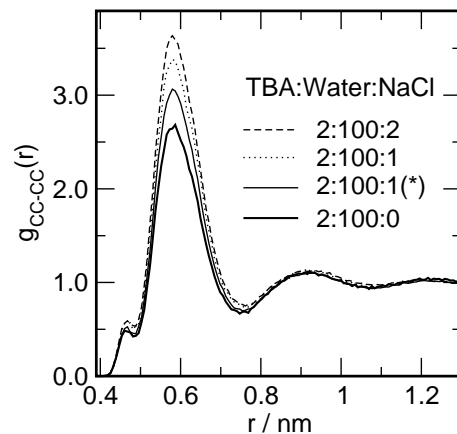


FIG. 1: Radial pair distribution functions between the TBA central carbon atoms (CC) in aqueous solutions at different salt concentrations. The star \* indicates the data belonging to parameter set of Koneshan et al [51] for NaCl.

TABLE IV: Coordination numbers for a 0.02 molar aqueous solution of t-butanol (TBA) with and without added sodium chloride. The coordination numbers are obtained by integrating over the distance interval indicated. For a direct comparison, the values of Ref. [25] were taken for  $r_{\min}$  and  $r_{\max}$ . CC-refers to the central carbon atom of TBA. OW denotes the Water-Oxygen while OH specifies the oxygen atom in the hydroxyl-group. The star\* indicates the parameter set for NaCl according to Koneshan et al. [51]. The neutron scattering data are taken from Ref. [25].

Atom-pair	$r_{\min}/\text{nm}$	$r_{\max}/\text{nm}$	TBA:Water:NaCl					
			2:100:0		2:100:1		MD sim.*	2:100:2
			n-scatt.	MD sim.	n-scatt.	MD sim.		MD sim.
CC-CC	0.43	0.75	$1.5 \pm 0.7$	$1.15 \pm 0.01$	$0.8 \pm 0.5$	$1.32 \pm 0.05$	$1.27 \pm 0.01$	$1.45 \pm 0.03$
CC-CC	0.75	1.00	$1.0 \pm 0.6$	$1.41 \pm 0.02$	$1.8 \pm 0.8$	$1.39 \pm 0.06$	$1.39 \pm 0.02$	$1.40 \pm 0.04$
OH-OH	0.25	0.35	$0.02 \pm 0.08$	$0.042 \pm 0.001$	...	$0.047 \pm 0.002$	$0.043 \pm 0.002$	$0.048 \pm 0.001$
OH-OW	0.25	0.35	$2.5 \pm 0.6$	$3.017 \pm 0.002$	$2.4 \pm 0.6$	$2.975 \pm 0.005$	$2.992 \pm 0.002$	$2.950 \pm 0.002$
Na-OW	0.21	0.30	...	...	$4.2 \pm 1.1$	$5.562 \pm 0.004$	$5.582 \pm 0.003$	$5.454 \pm 0.002$
Cl-OW	0.28	0.36	...	...	$4.9 \pm 1.3$	$5.715 \pm 0.003$	$6.319 \pm 0.003$	$5.629 \pm 0.002$
OH-Na	0.32	0.55	...	...	$0.2 \pm 0.2$	$0.098 \pm 0.001$	$0.101 \pm 0.001$	$0.191 \pm 0.002$
OH-Cl	0.29	0.38	...	...	$0.2 \pm 0.2$	$0.0120 \pm 0.0002$	$0.0134 \pm 0.0003$	$0.0251 \pm 0.0004$
HO-Cl	0.19	0.32	...	...	$0.04 \pm 0.07$	$0.0135 \pm 0.0003$	$0.0141 \pm 0.0003$	$0.0279 \pm 0.0004$

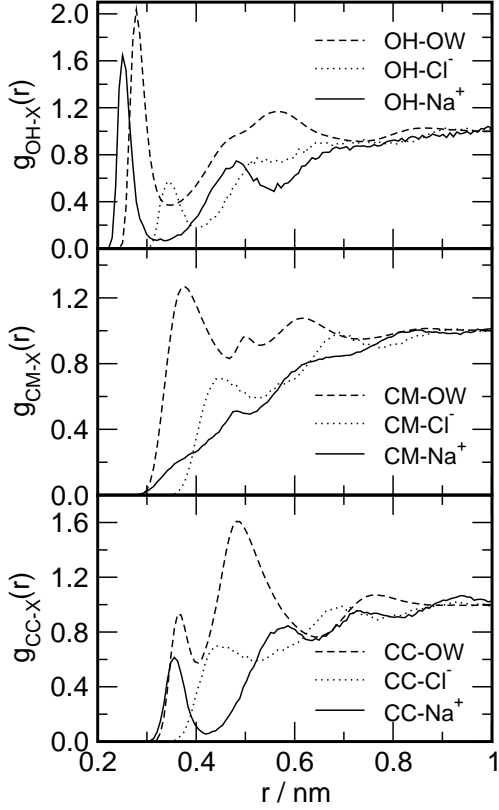


FIG. 2: Several representative TBA-solvent pair atom-atom radial distribution functions obtained from the TBA:Water:NaCl 2:100:1 solution. CC denotes the TBA central carbon atom, whereas CM and OH specify the methyl-carbon and hydroxyl oxygens, respectively.

a central TBA molecule is shown in Figure 4. The radial pair distribution functions in Figure 1 and the 2d-distributions in Figure 4 are interrelated and the radial

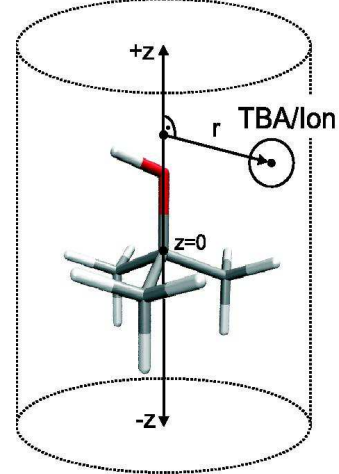


FIG. 3: Schematic illustration of the two-dimensional cylindrical pair distribution functions. Distribution of TBA and the ions around a central TBA molecule. The center of mass of the central TBA molecules is at  $(z = 0, r = 0)$  and the C-O-bond is aligned along the  $z$ -axis.

distribution functions can be obtained by averaging over angles  $\theta = \arctan(r/z)$ . Figure 4 reveals that the prepeak in the CC-CC radial pair distribution function located at about 0.47 nm is due to hydrogen bonded TBA-TBA pairs. These pairs are identified by a separate dark spot at about  $r = 0.3$  nm and  $z = 0.35$  nm in close proximity to the hydroxyl-group in Figures 4a and 4b. As deduced from the radial distribution functions in Figure 1, the addition of salt leads to an increased aggregation of TBA. The difference between the two-dimensional distribution functions with and without salt, shown in Figure 4c, reveals that aggregation occurs predominantly on the methyl-group side of the TBA molecule: The region with

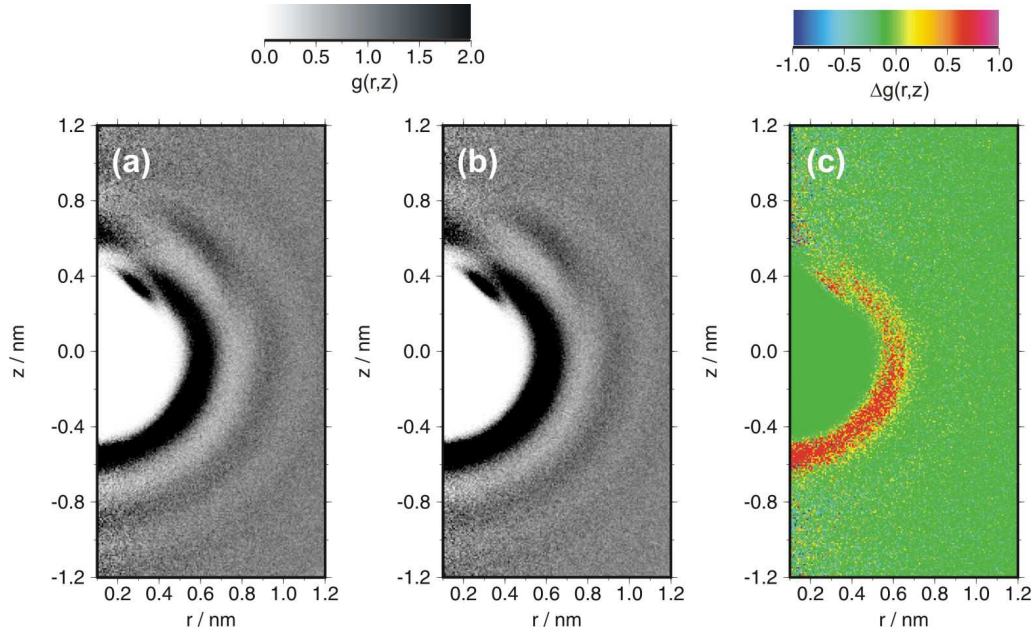


FIG. 4: Two dimensional cylindrical center of mass pair distribution functions  $g(r, z)$  of TBA around a central TBA-molecule with the C-O-Vector pointing upwards. (a) 2 TBA : 100 Water. (b) 2 TBA : 100 Water : 1 NaCl; (c) Difference between the distribution functions shown in (b) and (a) (salt minus no salt).

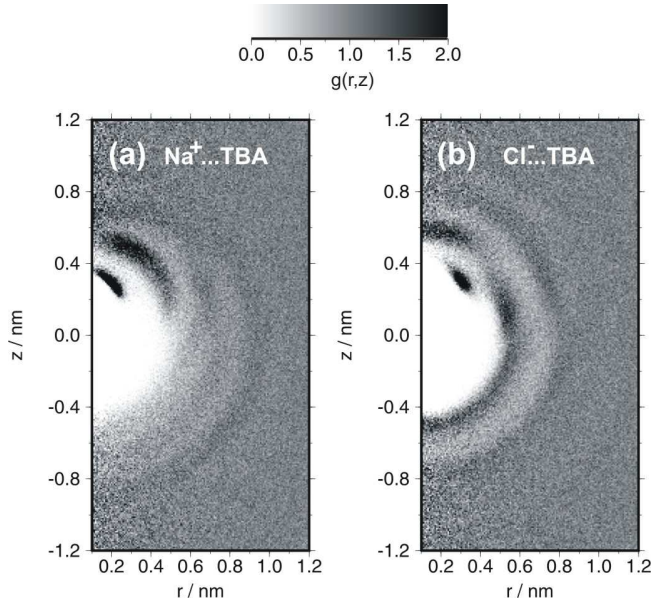


FIG. 5: Two dimensional cylindrical pair distribution functions  $g(r, z)$  of the sodium (a) and chloride (b) ions around a central TBA-molecule with the C-O-Vector pointing upwards. From the simulation with composition TBA:Water:NaCl of 2:100:1.

negative  $z$  shows an increase in peak height of about 0.5, whereas on the hydrophilic side, the peak heights remain almost unchanged.

The distributions of the ions around a TBA-molecule are shown in Figure 5. Dark regions close to the hydroxyl

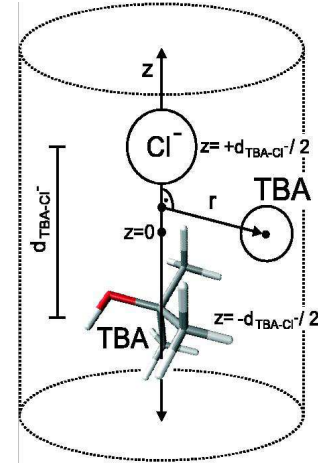


FIG. 6: Schematic illustration of the two-dimensional cylindrical pair distribution function  $g(r, z)$  of TBA molecules around a TBA -  $\text{Cl}^-$  contact pair with  $d_{\text{TBA-Cl}^-} < 0.64$  nm. The origin ( $z=0, r=0$ ) is located halfway between the centers of mass of TBA and  $\text{Cl}^-$ . The vector connecting TBA and  $\text{Cl}^-$  is aligned along the z-axis.

group indicate a significant stability of TBA-ion complexes. A remarkable difference is observed for adsorption of the different ions at the aliphatic side of TBA. The chloride ions tend to adsorb close to the Methyl-groups and are present as a grey shadow on the hydrophobic side of the TBA molecule as shown in Figure 5b, whereas the sodium completely tends to avoid that region. Consequently, there is practically no peak in the methyl-carbon-sodium radial pair correlation function in Figure



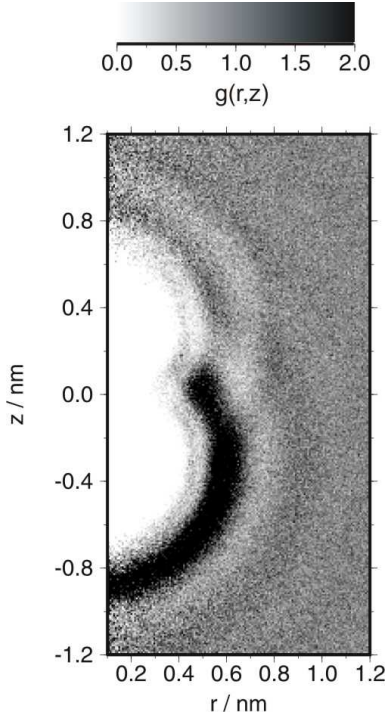


FIG. 7: Cylindrical pair distribution function TBA around a contact pair formed by a TBA-molecule and a Chloride ion (TBA:bottom;  $\text{Cl}^-$ : top). The geometry and the definition of  $r$  and  $z$  is indicated in Figure 6.

2. This observation seems to be in line with the recently reported selective chloride-adsorption at the liquid-gas interface [69, 70, 71], which has structural similarities with the interface to a hydrophobic surface [11, 72, 73].

In order to check whether there is a significant amount of chloride-bridged TBA-TBA configuration we calculate the two-dimensional cylindrical (TBA- $\text{Cl}^-$ )...TBA correlation functions of a second TBA molecule around a TBA- $\text{Cl}^-$  contact pair with a center of mass distance less than 0.64 nm according to

$$g(r, z) = \frac{1}{N_{\text{TBA-Cl}} \rho_{\text{TBA}}} \left\langle \sum_{i=1}^{N_{\text{TBA-Cl}}} \sum_{j=1}^{N_{\text{TBA}}} \delta(z - \vec{n}_{\text{TBA-Cl}} \vec{r}_{ij}) \times \delta\left(r - \sqrt{r_{ij}^2 - (\vec{n}_{\text{TBA-Cl}} \vec{r}_{ij})^2}\right) \right\rangle. \quad (14)$$

Here  $\vec{n}_{\text{TBA-Cl}}$  is the unit vector describing the orientation of a TBA- $\text{Cl}^-$  contact pair. An illustration is given in Figure 6. As can be seen clearly from Figure 7, the vast amount of TBA molecules is located on the TBA-side of the TBA- $\text{Cl}^-$ -pair, practically ruling out a significant contribution of TBA- $\text{Cl}^-$ -TBA bridges.

As the 2-dimensional cylindrical pair distribution functions indicate, the MD simulations furnish a scenario of an increased number of hydrophobic contacts in an aqueous solution of TBA in the presence of sodium chlo-

ride, in contrast to the observations of Bowron and Finney. However, when taking a look at the published data, and considering the given size of errorbars, the n-scattering and MD simulation are not at all contradictory. A quantitative comparison of the obtained coordination numbers is given in Table IV. Almost all indicated values agree within the given errors, or are at least very close to each other. In fact, the large error in the n-scattering data for the central carbon (CC) coordination numbers for the first and second hydration shell, probably forbids a clear distinction between both scenarios just relying on the n-scattering data. Taking the present MD simulation data into account, the hydrophobic association scenario seems to be the more likely variant.

Very recently Lee and van der Vegt have published a series of molecular dynamics simulations of TBA/water mixtures with varying composition [74]. In their study, using the SPC model for water, they find the OPLS potential for TBA less satisfactory and hence derive an improved set of model parameters for tertiary butanol. Lee and van der Vegt report a too strong association of the TBA molecules when using the original OPLS parameters, whereas our study reveals a far better (almost quantitative) agreement with experimental data. This apparent solvent-model dependence, however, is in line with the observed different strength of hydrophobic interaction obtained for simple solutes (noble gases) for the two water models. Paschek [75] found for the SPC model a substantially stronger hydrophobic association, which has also a significantly smaller temperature dependence. For our present study we choose the SPCE model since it describes a number of water properties more realistically than SPC [75, 76, 77], particularly the diffusion coefficient. However, using their model, preliminary data of Lee and van der Vegt also indicate an enhanced TBA-TBA association upon addition of sodium chloride [78].

## B. Self-Diffusion coefficients

We determined the self diffusion coefficients for all particle types in the MD simulation from the mean square displacement according to

$$D = \frac{1}{6} \lim_{t \rightarrow \infty} \frac{\partial}{\partial t} \langle |\vec{c}(t) - \vec{c}(0)|^2 \rangle, \quad (15)$$

where  $\vec{c}$  represents the position of the molecules center of mass. In fact, the diffusion coefficients are obtained from the slope of the mean square displacement over the time-interval between 100 ps and 500 ps. The lower boundary has been chosen to be large compared to the the average intermolecular association times. The diffusion coefficients obtained from the simulations are given in Table V. In addition, the the experimental self-diffusion coefficients for TBA-d1 in in heavy water/salt solutions are shown in Table III.

It is evident that the experimental diffusion coefficients of TBA are substantially smaller than the values obtained



TABLE V: Self diffusion coefficients  $D_{\text{self}}$  as obtained from the MD simulations for the TBA/Water- and TBA/Water/Salt-mixtures and for pure water.

Particle	$D/10^{-9} \text{ m}^2\text{s}^{-1}$				
	TBA:Water:NaCl				
	2:100:1*	2:100:2	2:100:1	2:100:0	0:100:0
H <sub>2</sub> O	$2.035 \pm 0.003$	$1.975 \pm 0.005$	$2.075 \pm 0.005$	$2.197 \pm 0.006$	$2.642 \pm 0.012$
TBA	$0.751 \pm 0.009$	$0.707 \pm 0.009$	$0.749 \pm 0.011$	$0.840 \pm 0.015$	
Na <sup>+</sup>	$0.987 \pm 0.018$	$1.041 \pm 0.013$	$1.091 \pm 0.017$		
Cl <sup>-</sup>	$1.200 \pm 0.021$	$1.162 \pm 0.014$	$1.290 \pm 0.020$		

TABLE VI: Parameters characterizing the H-H-dipolar correlation function for the TBA aliphatic hydrogen nuclei. The values indicate a by 20 % increased intermolecular relaxation rate  $(T_1^{-1})_{\text{inter}}$  in the presence of NaCl, whereas the intramolecular rate changes only by about 2 %. To obtain the correlation time  $\tau_2$ , the correlation function was integrated numerically while the tail of the correlation function was fitted to a single exponential function (inter: between 120 and 200 ps; intra: between 30 and 50 ps).

TBA:Water:NaCl	inter			intra		
	$\langle r_{\text{HH}}^{-6} \rangle / \text{nm}^{-6}$	$\tau_2 / \text{ps}$	$T_1 / \text{s}$	$\langle r_{\text{HH}}^{-6} \rangle / \text{nm}^{-6}$	$\tau_2 / \text{ps}$	$T_1 / \text{s}$
2 : 100	1667	8.89	79.0	76920	4.41	3.45
2 : 100 : 1	1739	10.25	65.7	74242	4.67	3.38
2 : 100 : 2	1958	10.61	56.3	74239	4.85	3.25
2 : 100 : 1*	1681	10.27	67.8	74249	4.68	3.37

from MD simulations. This has to be largely attributed to the fact that heavy water is used as a solvent in the experiment, which has a significantly smaller diffusion coefficient ( $D = 1.768 \times 10^{-9} \text{ m}^2\text{s}^{-1}$  at 298.25 K [79]) compared to H<sub>2</sub>O ( $D = 2.299 \times 10^{-9} \text{ m}^2\text{s}^{-1}$  at 298.2 K [68, 80]). However, even when taking this effect into account, the diffusion coefficient of TBA according to the MD simulations seems to be overestimated by about 40%, which could indicate an increased number of associated TBA-TBA pairs in the experiment. This discrepancy may at least partly also be attributed to a possible enhanced “retardation effect” [81] of heavy water in the hydrophobic hydration shell of TBA. The “retardation effect” is clearly seen in the simulations as the slowing down of the water molecules in the TBA/water solution. However, given that the water retardation effect is related to the structuring of water in the hydrophobic hydration shell, it is likely to be weaker in SPCE than in real water, since SPCE has been shown to underestimate the solvation entropy of hydrophobic particles [75].

In addition, we find that the decrease of the TBA diffusion coefficient upon addition of salt by 6.4% per  $\text{mol l}^{-1}$  NaCl is significantly smaller than by the 15.8% per  $\text{mol l}^{-1}$  NaCl as obtained in the MD simulation. The overestimated salt-effect might be attributed to the potentially too small diffusion coefficients observed for Na<sup>+</sup> and particularly Cl<sup>-</sup>. Scaling the ion self-diffusion coefficients with the diffusion coefficient of water in the

TBA/water system (as approximation), one would expect diffusion coefficients of  $D(\text{Na}^+) \approx 1.18 \times 10^{-9} \text{ m}^2\text{s}^{-2}$  and  $D(\text{Cl}^-) \approx 1.70 \times 10^{-9} \text{ m}^2\text{s}^{-2}$  for the  $c(\text{NaCl}) = 1.0 \text{ mol l}^{-1}$  concentration (using diffusion coefficients from Ref. [82] for the ions in aqueous solutions at the given concentration for 25°C). Although the interaction with the TBA molecules might also have a non-negligible effect, the MD simulations seem to underestimate the self-diffusion coefficients of the ions by about 13% and 46%, respectively. To confirm this observation we have additionally calculated self-diffusion coefficients for a pure salt solution containing 500 SPCE molecules and 16 ion pairs at 298 K and 1 bar, with a concentration of 1.67 mol. We obtain diffusion coefficients of  $D(\text{Na}^+) = 1.07 \times 10^{-9} \text{ m}^2\text{s}^{-2}$ ,  $D(\text{Cl}^-) = 1.21 \times 10^{-9} \text{ m}^2\text{s}^{-2}$ , and  $D(\text{H}_2\text{O}) = 2.18 \times 10^{-9} \text{ m}^2\text{s}^{-2}$ . The diffusion coefficients of the ions clearly indicate that there is a need for improvement of the employed ion parameter sets. Particularly the hydration-strength of the chloride ion seems to be overestimated by the present models. The overall agreement with the n-scattering data and the less satisfactory diffusion data, however, might just reflect the more pronounced sensitivity of kinetic quantities on details of the pair correlation function, such as e.g. the first minimum in the ion-water pair correlation function. This property is critically related to the water-exchange rate, but is probably just not resolved accurate enough in the n-scattering data. When comparing the diffusion coeffi-

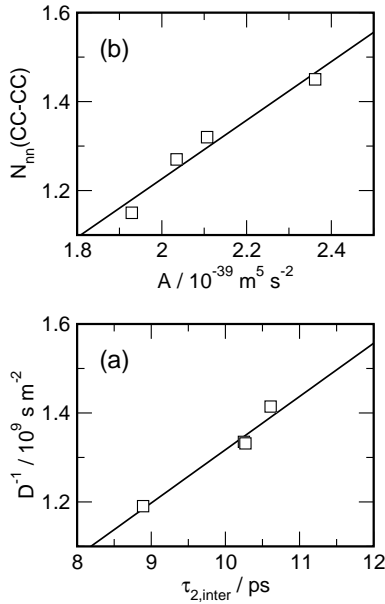


FIG. 8:  $A$ -parameter related-quantities as obtained from the MD-simulation: a) Inverse self-diffusion coefficient of TBA  $D^{-1}$  versus the intermolecular dipolar correlation time  $\tau_{2,\text{inter}}$  of the aliphatic protons in TBA for the different MD simulations. b) TBA-TBA aliphatic carbon coordination number versus the  $A$ -parameter.

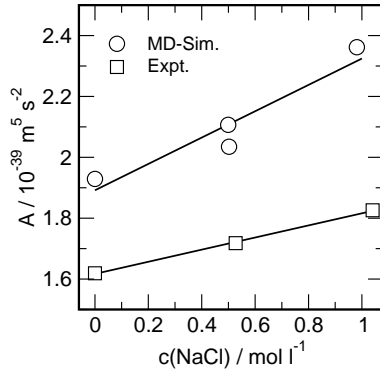


FIG. 9:  $A$ -parameter obtained from MD simulation and experiment as a function of salt concentration.

cients according to the different ion parameter sets shown in Table V, the Koneshan et al. parameters seem to be even less satisfactory than the Heinzinger parameters.

### C. TBA-TBA association and the $A$ -parameter

Given the uncertainties in the employed potential parameter sets, we have tried to find more experimental evidence for an enhanced hydrophobic association, as it is found in our MD simulations. Therefore we perform nuclear magnetic relaxation experiments on aqueous solutions of tertiary butanol with varying salt concentration while keeping the butanol concentration con-

stant. Given a non-changing intermolecular dipolar correlation time  $\tau_{2,\text{inter}}$ , an increasing relaxation rate would directly indicate an association behavior as observed in our MD-simulations, whereas a decreasing relaxation rate would support the scenario obtained by Bowron and Finney. However, since the correlation times are likely to be changing we follow the  $A$ -parameter approach proposed by Hertz and co-workers, discussed extensively in a separate section above. The  $A$ -parameter approach is based on the assumption of a linear relationship between the intermolecular dipolar relaxation time  $\tau_{2,\text{inter}}$  and the inverse self-diffusion coefficient of the solute molecules, which can be obtained independently. Hence we have calculated the inter- and intramolecular dipole-dipole correlation functions for the aliphatic hydrogens for all MD-simulations, assuming that all other protons are exchanged by deuterons. Moreover, only like-spin  $^1\text{H} - ^1\text{H}$  dipolar interactions were considered in the calculations. A quantitative description of the intra- and intermolecular contributions as well as the calculated relaxation times  $T_1$  are given in Table VI. The TBA self-diffusion coefficients for each of the simulated systems is given in Table V. Figure 8 shows that the intermolecular correlation times  $\tau_{2,\text{inter}}$  and the inverse self diffusion coefficient of TBA are indeed almost linearly related, suggesting that the  $A$ -parameter approach might be a useful approximation in the present case. Moreover, the obtained  $A$ -parameter is also almost linearly related to the TBA-TBA coordination number, proposing an interpretation of the  $A$ -parameter as an approximate measure of the TBA-TBA coordination number. The  $A$ -parameters obtained experimentally from the measured diffusion coefficients and relaxation rates are given in Table III. Both experimental and simulated  $A$ -Parameters are shown in Figure 9. We would like to point out the almost linear relationship remains to be true even when changing the sodium chloride intermolecular potentials. Changing diffusion coefficients are apparently counterbalanced by also changing aggregation numbers. Although we cannot fully rule out that this finding might just be fortuitous, we take the linear relationship to determine approximate TBA-TBA coordination numbers as well from the experimental data. Doing so, we get coordination numbers of  $N_{nn}(\text{TBA}) = 0.975, 1.040$ , and  $1.111$  for the solutions with concentrations  $0.0 \text{ mol l}^{-1}$ ,  $0.5270 \text{ mol l}^{-1}$ , and  $1.0403 \text{ mol l}^{-1}$ , respectively. Although, significantly smaller than the coordination numbers obtained from MD-simulation, and suggesting a smaller concentration variation, the experimentally obtained  $A$ -parameters and coordination numbers tend to suggest an enhanced hydrophobic aggregation of the TBA molecules with increasing salt concentration. Finally, we would like to point out that the “experimental” coordination numbers agree well with the n-scattering data shown in Table IV.

#### IV. CONCLUSIONS

We have used a combination of molecular dynamics simulations and nuclear magnetic relaxation measurements to investigate the effect of salt (sodium chloride) on the association-behavior of tertiary butanol molecules in an aqueous solution. We have shown that the so-called “*A*-parameter” proposed by Hertz and co-workers as measure for the degree of association of solute molecules in aqueous solution is a well justified quantity in the present case. MD-simulation establish an almost linear relationship between the *A*-parameter and the TBA-TBA coordination numbers. The relationship remains independent from changes of potential-parameters for sodium chloride. Both theory and experiment support the more intuitive view of an enhanced number of hydrophobic contacts between TBA-molecules in the presence of salt. Moreover, an increasing salt concentration is found to further strengthen the solute-solute hydrophobic interaction. The TBA molecules are therefore behaving closely

similar to purely hydrophobic solutes [8]. A detailed structural characterization of the MD-simulation data does hence not provide evidence for a significant amount of chloride-bridged butanol-pairs, as recently proposed from the analysis of neutron experiments [24, 25]. Finally, although our results suggest a structurally completely distinct scenario, the molecular dynamics simulations, as well as the coordination numbers according to the NMR-experiments, appear to be largely within the experimental errorbars of the Bowron and Finney work [25].

#### Acknowledgments

We acknowledge support from the Deutsche Forschungsgemeinschaft (FOR-436 and GK-298) and the University of Dortmund (“Forschungsband Molekulare Aspekte der Biowissenschaften”). The authors are grateful to M. Holz for critically reading the manuscript.

- 
- [1] C. Tanford, *The Hydrophobic Effect: Formation of Micelles and Biological Membranes* (John Wiley & Sons, New York, 1980), 2nd ed.
  - [2] A. Ben-Naim, *Hydrophobic Interactions* (Plenum Press, New York, 1980).
  - [3] L. R. Pratt, *Annu. Rev. Phys. Chem.* **53**, 409 (2002).
  - [4] N. T. Southall, K. A. Dill, and A. D. J. Haymet, *J. Phys. Chem. B* **106**, 521 (2002).
  - [5] B. Widom, P. Bhimalapuram, and K. Koga, *Phys. Chem. Chem. Phys.* **5**, 3085 (2003).
  - [6] W. L. Masterton, D. Bolocofsky, and T. P. Lee, *J. Phys. Chem.* **75**, 2809 (1971).
  - [7] M. Kinoshita and F. Hirata, *J. Chem. Phys.* **106**, 5202 (1997).
  - [8] T. Ghosh, A. E. García, and S. Garde, *J. Phys. Chem. B* **107**, 612 (2003).
  - [9] T. Ghosh, A. Kalra, and S. Garde, *J. Phys. Chem. B* **109**, 642 (2005).
  - [10] K. Koga, *J. Chem. Phys.* **121**, 7304 (2004).
  - [11] D. Huang and D. Chandler, *Proc. Natl. Acad. Sci. USA* **97**, 8324 (2000).
  - [12] H. S. Ashbaugh and L. R. Pratt, physics/0307109v2.
  - [13] D. Chandler (2005), Nature insight review article (preprint).
  - [14] M. Holz and M. Sørensen, *Ber. Bunsenges. Phys. Chem.* **96**, 1441 (1992).
  - [15] M. Holz, R. Grunder, A. Sacco, and A. Meleleo, *J. Chem. Soc. Faraday Trans.* **89**, 1215 (1993).
  - [16] A. Sacco, F. M. De Cillis, and M. Holz, *J. Chem. Soc. Faraday Trans.* **94**, 2089 (1998).
  - [17] M. Mayele, M. Holz, and A. Sacco, *Phys. Chem. Chem. Phys.* **1**, 4615 (1999).
  - [18] M. Mayele and M. Holz, *Phys. Chem. Chem. Phys.* **2**, 2429 (2000).
  - [19] G. W. Euliss and C. M. Sorensen, *J. Chem. Phys.* **80**, 4767 (1984).
  - [20] D. T. Bowron, J. L. Finney, and A. K. Soper, *J. Phys. Chem. B* **102**, 3551 (1998).
  - [21] D. T. Bowron, A. K. Soper, and J. L. Finney, *J. Chem. Phys.* **114**, 6203 (2001).
  - [22] D. T. Bowron and J. L. Finney, *Phys. Rev. Lett.* **89**, 215508 (2002).
  - [23] S. Dixit, J. Crain, W. C. K. Poon, J. L. Finney, and A. K. Soper, *Nature (London)* **416**, 829 (2002).
  - [24] D. T. Bowron and S. Díaz Moreno, *J. Chem. Phys.* **117**, 3753 (2002).
  - [25] D. T. Bowron and J. L. Finney, *J. Chem. Phys.* **118**, 8357 (2003).
  - [26] M. G. Cacace, E. M. Landau, and J. J. Ramsden, *Q. Rev. Biophys.* **30**, 241 (1997).
  - [27] F. Hofmeister, *Arch. Exp. Path. Pharmacol.* **24**, 247 (1888).
  - [28] V. A. Parsegian, *Nature (London)* **378**, 335 (1995).
  - [29] B. Hribar, N. T. Southall, V. Vlachy, and K. A. Dill, *J. Am. Chem. Soc.* **124**, 12302 (2002).
  - [30] A. Geiger, *Ber. Bunsenges. Phys. Chem.* **85**, 52 (1981).
  - [31] R. Leberman and A. K. Soper, *Nature (London)* **378**, 364 (1995).
  - [32] J. L. Finney and A. K. Soper, *Chem. Soc. Rev.* **23**, 1 (1994).
  - [33] A. K. Soper, *Chem. Phys.* **202**, 295 (1996).
  - [34] A. K. Soper, *Mol. Phys.* **99**, 1503 (2001).
  - [35] D. T. Bowron, *Philos. T. Roy. Soc. b* **359**, 1167 (2004).
  - [36] J. L. Finney and D. T. Bowron, *Curr. Opin. Colloid. In.* **9**, 59 (2004).
  - [37] J. L. Finney and D. T. Bowron, *Philos. T. Roy. Soc. A* **363**, 469 (2004).
  - [38] M. G. Burke, R. Woscholski, and S. N. Yaliraki, *Proc. Natl. Acad. Sci. USA* **100**, 13928 (2003).
  - [39] H. G. Hertz, *Prog. NMR Spec.* **3**, 159 (1967).
  - [40] H. G. Hertz and R. Tutsch, *Ber. Bunsenges. Phys. Chem.* **80**, 1268 (1976).
  - [41] A. Abragam, *The Principles of Nuclear Magnetism* (Oxford University Press, 1961).

- [42] P. Westlund and R. Lynden-Bell, *J. Magn. Reson.* **72**, 522 (1987).
- [43] M. Odelius, A. Laaksonen, M. H. Levitt, and J. Kowalewski, *J. Magn. Reson. Ser. A* **105**, 289 (1993).
- [44] E. O. Stejksal, D. E. Woessner, T. C. Farrar, and H. S. Gutowsky, *J. Chem. Phys.* **31**, 55 (1959).
- [45] P. A. Egelstaff, *An Introduction to the Liquid State* (Oxford University Press, Oxford, 1992), 2nd ed.
- [46] A. L. Capparelli, H. G. Hertz, and R. Tutsch, *J. Phys. Chem.* **82**, 2023 (1978).
- [47] K. J. Müller and H. G. Hertz, *J. Phys. Chem.* **100**, 1256 (1996).
- [48] K. J. Müller and H. G. Hertz, *J. Phys. Chem.* **100**, 1256 (1996).
- [49] U. Wandle and H. G. Hertz, *Z. Phys. Chem.* **178**, 217 (1992).
- [50] K. Heinzinger, in *Computer Modelling of Fluids Polymers and Solids*, edited by C. R. A. Catlow, S. C. Parker, and M. P. Allen (Kluwer Academic Publishers, Dordrecht, 1990), vol. C293 of *NATO ASI Series*, pp. 357–369.
- [51] S. Koneshan, J. C. Rasaiah, R. M. Lynden-Bell, and S. H. Lee, *J. Phys. Chem. B* **102**, 4193 (1998).
- [52] S. Nosé, *Mol. Phys.* **52**, 255 (1984).
- [53] W. G. Hoover, *Phys. Rev. A* **31**, 1695 (1985).
- [54] M. Parrinello and A. Rahman, *J. Appl. Phys.* **52**, 7182 (1981).
- [55] S. Nosé and M. L. Klein, *Mol. Phys.* **50**, 1055 (1983).
- [56] U. Essmann, L. Perera, M. L. Berkowitz, T. A. Darden, H. Lee, and L. G. Pedersen, *J. Chem. Phys.* **103**, 8577 (1995).
- [57] S. Miyamoto and P. A. Kollman, *J. Comp. Chem.* **13**, 952 (1992).
- [58] J. P. Ryckaert, G. Ciccotti, and H. J. C. Berendsen, *J. Comp. Phys.* **23**, 327 (1977).
- [59] E. Lindahl, B. Hess, and D. van der Spoel, *J. Mol. Model.* **7**, 306 (2001).
- [60] D. van der Spoel, E. Lindahl, B. Hess, A. R. van Buuren, E. Apol, P. J. Meulenhoff, D. P. Tieleman, A. L. T. M. Sijbers, K. A. Feenstra, R. van Drunen, et al., *Gromacs User Manual version 3.2*, [www.gromacs.org](http://www.gromacs.org) (2004).
- [61] D. Paschek, *MOSCITO4 molecular dynamics simulation package* (2005), ([www.moscitomd.de](http://www.moscitomd.de)).
- [62] H. Flyvbjerg and H. G. Petersen, *J. Chem. Phys.* **91**, 461 (1989).
- [63] H. J. C. Berendsen, J. P. M. Postma, W. F. van Gunsteren, A. DiNola, and J. R. Haak, *J. Chem. Phys.* **81**, 3684 (1984).
- [64] H. J. C. Berendsen, J. R. Grigera, and T. P. Straatsma, *J. Phys. Chem.* **91**, 6269 (1987).
- [65] W. L. Jorgensen, D. S. Maxwell, and J. Tirado-Rives, *J. Am. Chem. Soc.* **118**, 11225 (1996).
- [66] G. Bonera and A. Rigamonti, *J. Chem. Phys.* **42**, 171 (1965).
- [67] W. S. Price, *Concepts Magn. Reson.* **10**, 197 (1998).
- [68] R. Mills, *J. Chem. Phys.* **77**, 685 (1973).
- [69] E. M. Knipping, M. J. Lakin, K. L. Foster, P. Jungwirth, D. J. Tobias, R. B. Gerber, D. Dabdub, and B. J. Finlayson-Pitts, *Science* **288**, 301 (2000).
- [70] P. Jungwirth and D. J. Tobias, *J. Phys. Chem. B* **104**, 7702 (2000).
- [71] P. Jungwirth and D. J. Tobias, *J. Phys. Chem. B* **105**, 10468 (2001).
- [72] H. A. Patel, E. B. Naumann, and S. Garde, *J. Chem. Phys.* **119**, 9199 (2003).
- [73] I. Brovchenko, A. Geiger, and A. Oleinikova, *J. Phys. Condens. Matt.* **16**, S5345 (2004).
- [74] M. E. Lee and N. F. A. van der Vegt, *J. Chem. Phys.* **122**, 114509 (2005).
- [75] D. Paschek, *J. Chem. Phys.* **120**, 6674 (2004).
- [76] G. Hura, J. M. Sorenson, R. M. Glaeser, and T. Head-Gordon, *J. Chem. Phys.* **113**, 9140 (2000).
- [77] J. M. Sorenson, G. Hura, R. M. Glaeser, and T. Head-Gordon, *J. Chem. Phys.* **113**, 9149 (2000).
- [78] N. F. A. van der Vegt (2005), private communication.
- [79] W. S. Price, H. Ide, Y. Arata, and O. Söderman, *J. Phys. Chem. B* **104**, 5874 (2000).
- [80] M. Holz, S. R. Heil, and A. Sacco, *Phys. Chem. Chem. Phys.* **2**, 4740 (2000).
- [81] R. Haselmeier, M. Holz, W. Marbach, and H. Weingärtner, *J. Phys. Chem.* **99**, 2243 (1995).
- [82] R. Mills and V. M. M. Lobo, *Self-diffusion in electrolyte solutions*, vol. 36 of *physical sciences data* (Elsevier, Amsterdam, The Netherlands, 1989).